CERN - EUROPEAN ORGANIZATION FOR NUCLEAR RESEARCH

Submitted to
Nuclear Physics B

CERN/EP/PHYS 78-14 Rev.
7 July 1978

QUANTUM NUMBER EFFECTS IN EVENTS WITH A CHARGED PARTICLE OF LARGE TRANSVERSE MOMENTUM

(PART 1: LEADING PARTICLES IN JETS)

CERN-Collège de France-Heidelberg-Karlsruhe Collaboration

D. DRIJARD, H.G. FISCHER, W. GEIST, R. GOKIELI[1], P.G. INNOCENTI, V. KORBEL[2], A. MINTEN, A. NORTON, R. SOSNOWSKI[1], S. STEIN[3], O. ULLALAND and H.D. WAHL
CERN, European Organization for Nuclear Research, Geneva, Switzerland

P. BURLAUD, M. DELLA NEGRA[4], G. FONTAINE, P. FRENKIEL, C. GHESQUIERE, D. LINGLIN[4] and G. SAJOT
Collège de France, Paris, France

H. FREHSE[5], E.E. KLUGE, A. PUTZER and J. STIEWE
Institut für Hochenergiephysik der Universität Heidelberg, Germany

P. HANKE[5], W. HOFMANN[6], W. ISENBECK, J. SPENGLER[6] and D. WEGENER[6]
Institut für experimentelle Kernphysik der Universität (TH) Karlsruhe, Germany

---

1 Now at Institute for Nuclear Research , Warsaw, Poland

2 Now at DESY, Hamburg, Germany

3 Now at SLAC, Stanford, USA

4 Now at LAPP, Annecy, France

5 Now at CERN, Geneva, Switzerland

6 Now at Institut für Physik, Universität Dortmund, Germany.

EEK/jm

ABSTRACT

In an experiment done with the SFM-facility at the CERN-ISR, we have studied events with a high p_T particle (π^+, π^-, K^-, p) produced at $\theta = 20^o$ and $\theta = 45^o$. The distribution of leading fragments of the spectator jet in the same rapidity hemisphere as the trigger depends strongly on the kind of trigger particle involved. These distributions agree with predictions from dimensional counting rules, if parton scattering via vector gluon exchange is assumed for the large p_T process. The average charge of the fastest particle (jet leader) in the away jet is $\simeq 1/3$ independent of the trigger charge, a value expected if 3 valence quarks participate in the hard scattering process. For transverse momenta of $\simeq 2$ GeV/c the $\rho^o/\pi^\pm$ production ratio is near unity.

1. INTRODUCTION

The phase space structure of secondaries in events with a particle of large transverse momentum can be adequately described within the framework of the parton model, as we have shown in a previous publication [1]. There we assumed that the underlying process is the elastic hard scattering of partons with transverse momentum k_T via vector gluon exchange. The subsequent fragmentation of the scattered partons and the unaffected partons ("spectators") gives rise to a four jet structure of the event as is sketched in fig. 1.

Whereas in ref. [1] our experimental data were analysed summing over the charges of the secondaries and irrespective of the nature of the triggering particle, we are going to differentiate here. By doing so, we shall be able to study whether the partons found to be responsible for the large p_T process are compatible with quarks. Making use of the known quark composition of the proton, distinctive predictions can be made on the quantum number structure of large p_T events. We shall in particular study the charge structure of secondaries accompanying the trigger particle of large p_T and the phase space population for different kinds of trigger particles involved.

The experiment was performed by triggering on large p_T charged particles at two different polar angle settings, $\theta \simeq 45^o$ and $\theta \simeq 20^o$. Selecting the unsusually asymmetric large p_T event configuration with a trigger angle $\theta \simeq 20^o$, the trigger jet and the spectator jet in the same rapidity hemisphere tend to originate from the same proton. This is so, whenever parton scattering yields a forward peaked angular distribution especially in our model [1]. Hence, the other incident proton produces the jet away in azimuth from the trigger and the spectator jet of rapidity opposite to the trigger. This situation is illustrated in fig. 1. Thus, no quantum number correlations are expected between the trigger particle and both opposite rapidity spectator and away side jets (besides kinematical effects due to parton distribution functions). One aim is to test this prediction. On the other hand, given the known composition of protons in terms of quark partons, correlations are expected between the quantum numbers of the

triggering particle and of the same rapidity spectator jet since both originate from the same proton. We will make use of quark fragmentation functions [2,3] and dimensional counting rules [4] to establish the quark parton content of the four jets and to test these predictions.

2. EXPERIMENTAL PROCEDURE

The Split Field Magnet (SFM) of the CERN Intersecting Storage Rings (ISR) allowed, in nearly the full solid angle, to measure charge and momenta of the particles produced in pp interactions at $\sqrt{s}$ = 52.2 GeV. An efficient trigger road through the chamber system was set up containing the trajectories of charged particles with a large transverse momentum in a given polar angular region ($\theta = 20^{\circ}$ or $\theta = 45^{\circ}$), using the selftriggering properties of the Multiwire Proportional Chamber (MWPC) system. Details of the set-up, of the acceptance, the resolution and the data analysis procedure have been described in [1].

A data sample with large p_T positive particles at $\theta = 20^{\circ}$ was obtained in an angular region of the trigger which was covered by threshold Cerenkov counters filled with freon-12 to detect π^+ mesons by their Cerenkov light [5]. The trigger particle of large p_T was required to have total momentum p > 7 GeV. This ensures a Cerenkov counter efficiency of > 99,6% for the detection of π-mesons. Hence, the admixture of π^+-mesons in the sample of events with a positive trigger particle which produced no light "K^+/p sample" was (1 ± 1)%. Because of the small production angle of $\theta = 20^{\circ}$ the ratio of protons to all positive particles in the "K^+/p sample" is in the order of 80% [6], therefore the K^+/p sample in the following is referred to as the proton trigger.

A sample of events with a negative trigger particle of p_T > 1.4 GeV not producing light in the threshold Cerenkov counters was also obtained. K^-mesons contribute to more than 70% to this sample [6], hence we assume in the following that this data set is characteristic for a K^- meson trigger. The admixture of π^--mesons to this sample is smaller than 5%.

For the event sample with a negative trigger particle at $\theta = 20^{\circ}$ and $p_T > 2$ GeV no particle identification was possible in the present experiment. Since π^--mesons dominate the negative particle production process at these angles [7], we assume that the negative trigger particle at $\theta = 20^{\circ}$ is a π^--meson.

In the following the secondary particles are described in the proton-proton center of mass system by their rapidity y or their reduced longitudinal momentum (Feynman variable) x, their azimuthal angle θ and their transverse momentum p_T. The coordinate system used is shown in fig. 2. The data sample has been corrected for acceptance losses and a transverse momentum cut for charged secondaries of $p_T > 0.25$ GeV/c has been applied.

3. PROPERTIES OF THE SPECTATOR JETS

The large p_T process depicted in fig. 1 yields two spectator jets, one originating from the same proton as the triggering particle, the second one from the other proton. The directions of the two spectator jets coincide approximately with the directions of the respective incident protons. The asymmetric trigger condition $\theta \simeq 20^{\circ}$ ensures that the trigger particle and the spectator jet in the same rapidity hemisphere originate from the same proton [1]. The second proton then produces the jet "away" in azimuth and the spectator in the opposite rapidity hemisphere, fig. 1. Having identified the triggering large p_T particle, we wish to see in which way the event structure depends on the trigger properties. In fig. 3 we show the ratio of the rapidity distributions of positive secondary particles for a π^+ trigger to the one with a π^- trigger and similarly for negative secondaries.

Since in our set up the π^+ trigger is at $\phi = 0^{\circ}$ and the π^- trigger is at $\phi = 180^{\circ}$, we include only secondaries in an azimuthal angular region symmetrical to both, namely $\phi = 90^{\circ} \pm 40^{\circ}$ and $\phi = 270^{\circ} \pm 40^{\circ}$. This cut also ensures that particles originate mostly from the spectator jets.

In a way similar to fig. 3, fig. 4 gives the ratio of the rapidity distributions of particles associated to p and π^+ trigger and correspondingly fig. 5 for K^- and π^- trigger.

3.1 Opposite rapidity spectator jet

As pointed out above, no quantum number correlations are expected between the trigger particle and the opposite rapidity spectator jet, if vector gluon exchange is the dominant mechanism for large p_T processes. We test one aspect of this prediction by studying the charge composition of the secondaries. As is evident from figs 3, 4 and 5 the rapidity distributions of positive and negative particles in the opposite rapidity hemisphere are indeed independent of the nature of the trigger particle. It should be noticed that the rapidity ranges of the trigger jet and of the away side jet do not extend beyond $y < -2$ (see also fig. 5 of [1]).

3.2 Same rapidity spectator jet

As can be seen in figs 3, 4 and 5, there exist correlations between the nature of the trigger particle and the charge of secondaries. The charge ratios deviate markedly from unity for $y > 2$, the rapidity range dominated by particles from the same side spectator jet.

This deviation is present in the whole kinematically allowed same rapidity range. Thus it cannot be attributed to the away side jet whose distribution is symmetrical in rapidity [1] and limited to the range with $|y| < 2$. We therefore are going to study whether this structure is due to quantum number correlation between the trigger particle and its spectator.

Triggering on single particles of large p_T we select trigger jets where a single particle takes nearly the full jet momentum [8]. Thus an idenfification of the fragmenting quark is possible and we see that e.g. π^+ stem from u-quarks, π^- from d-quarks and K^--mesons from sea quarks [2].

Taking into account the quark composition of the incident proton, we then know which quarks remain in the spectator system of the same rapidity hemisphere (fig. 1). For the fragmentation of these quarks we can predict the scaling behaviour of particle densities, e.g. by quark counting rules and compare the expected distributions of fast particles with the observed ones. This allows a further investigation of the underlying hard scattering process.

For this purpose we have to establish the proper scaling variable for the fragmentation of the spectator jet, since in large p_T events the available energy of the spectator system is reduced when compared to the pp c.m.s. energy. Hence the usual Feynman variable x ($= p_L/p_{Lmax}$) is not suitable to describe spectator fragmentations.

We therefore define for the system of the two spectator jets, which moves with a momentum p' in the proton-proton restframe, a reduced energy $\sqrt{s}'$ (neglecting parton k_T). Denoting by y_1 and y_2 the rapidities of the trigger jet and the away side jet, the overall energy momentum and invariant mass of the spectator system are

$$E' = \sqrt{s} - m_T(\cosh y_1 + \cosh y_2)$$

$$p' = \quad - m_T(\sinh y_1 + \sinh y_2)$$

Here m_T is the transverse mass of the jet (i.e. $m_{T1} = m_{T2}$).

We use the following approximations for y_1, y_2 and m_T:

$$y_1 = y^{(t)}, \quad ((t) = \text{Trigger})$$

$$y_2 = 0, \quad (\text{experimentally: } \langle y_2 \rangle = 0.05)$$

$$m_T = 1.1 \cdot p_T^{(t)}.$$

The resulting scaling variable, the reduced longitudinal momentum of a secondary in the c.m. system of the two spectators, is then

$$x' = 2p_y'/\sqrt{s}'.$$

Since inclusive particle spectra resulting from quark fragmentation are expected to show a power law behaviour $(1 - x')^n$ for $x' \to 1$ [4], we present in figs 6 to 10 the quantity $x' \cdot dN/dx'$ versus $(1 - x')$ (or ratios thereof) on a double logarithmic scale. The distributions are given for different combinations of trigger particle and charge of secondaries in the spectator jet. As can be observed in the figures, the distributions show marked differences and we shall try to explain these at least qualitatively.

To estimate the expected power behaviour of the fragmentation function, we make use of dimensional counting rules [4], according to which the inclusive distribution of hadrons from the fragmentation of a system of quarks is given by $xd\sigma/dx \sim (1 - x)^{2n-1}$, where n is the number of quarks remaining in the system after emission of the hadron under consideration. In table 1 we give the expected power law behaviour depending on the quantum numbers of the trigger and the associated secondaries. Counting rules yield identical results for the distribution functions $u(x)$ and $d(x)$ for u and d quarks and for their fragmentation into π^+ and π^- respectively. In inelastic pp collisions a reduced longitudinal momentum distribution of $\simeq (1 - x)^3$ for π^+ and $\simeq (1 - x)^4$ for π^- is observed [9]. Therefore, we increase the predicted power by one, whenever a valence d quark is fragmenting. Moreover, for the cases of meson triggers and positive secondaries in the spectator jet the latter are taken to be protons. Counting rule predictions for different combinations of trigger particle and spectator fragment type are given in table 1. Since the variable x' is only an approximation to the correct scaling variable, the counting rule predictions should not be taken too literally. Furthermore, with increasing power n, the experimental distributions fall quite rapidly for $x' \to 1$ and hence the statistical accuracy becomes rather limited.

As a first example we display in fig. 6 the x' distribution of positive secondaries in the spectator jet for the case of a proton trigger. Also shown is the fragmentation function $x'D_u^{\pi^+}(x')$, [3], which is seen to describe the experimental x' dependence quite well. Dimensional counting rules yield a prediction very similar to the function $x'D_u^{\pi^+}(x')$, namely

$(1 - x')$, if we assume that the spectator consists of a single quark (i.e. the trigger proton taking two quarks from the incident proton).

The next example in fig. 7 shows for a pion trigger the x' distribution of positive secondaries in the spectator jet, which we can safely assume to be mainly protons. The distribution is quite similar to the one in fig. 6, in fact dimensional counting rules predict the same behaviour for the fragmentation of an (ud) diquark system into a proton as for as u quark into a π^+. Thus we compare the data with the same fragmentation function $x'D_u^{\pi^+}$ as in the previous case.

Fig. 8 shows the x' distribution of negative secondaries for a π^+ trigger, quite different from the previous two fragmentation distributions. In this case a diquark system fragments into a pion and no fragmentation functions are available for comparison. Thus we make use of the modified dimensional counting rules of table 1, giving a $(1 - x')^4$ behaviour for a π^- in the spectator jet, which is seen to reproduce the data.

Similarly in fig. 9 ratios of x' distributions for secondaries in the spectator jet associated to a π^- trigger and to a π^+ trigger are shown both for positive and negative secondaries. Again a comparison is made with counting rules and good agreement is observed.

Fig. 10 is the ratio of x' distribution of K^- triggered to π^- triggered positive and negative secondaries in the spectator jet. Again experimental distributions agree with counting rule predictions, if we assume triggering K meson to originate from a scattered sea quark.

Finally, in fig. 11 the negative to positive spectator particle ratio for a proton trigger is shown as a function of x' and compared to counting rule predictions.

It should be pointed out, that in the case of the proton trigger, the inclusive distributions of particles in the spectator jet are in agreement with simple predictions only if single quark fragmentation is assumed. Diquark and gluon fragmentation are excluded by the data. We are therefore led to conclude, that the triggering proton contains two valence quarks from the incident proton. Hence one would speculate that either two quarks

are affected by the hard scattering process or our forward trigger condition, $\theta = 20^{o}$, in the p_T range under consideration, is fulfilled by a proton coming from a spectator jet (which recoils with transverse momentum k_T [1]).

4. TRIGGER JET PROPERTIES

As pointed out, triggering on single charged particles, the well known "trigger bias" [8] is present in our data, resulting in the fact, that the trigger takes nearly all of the scattered quarks momentum.

Here we study the question whether the triggering large p_T particle is always a first generation fragmentation product of the hard scattered parton. We shall specifically determine the ratio of charged pions to ρ^{o} mesons with the same p_T value. Both because of theoretical arguments concerning the symmetry of diquark systems and because of experimental results in deep inelastic electron scattering [10], this ratio is expected to be near unity. Note however, that even for a ρ/π ratio of one, only a small fraction of the observed pions stem from ρ decay due to the steep fall off in transverse momentum. To measure the ρ/π ratio we use our data at $\theta = 20^{o}$, where π^{+} and π^{-} are identified by the Cerenkov counters. To establish the presence of a ρ meson, we compute the invariant mass of the trigger with any charged particle of opposite sign in an azimuthal range of $\Delta\phi = \pm 40^{o}$ around the trigger.

In figs 12(a,b) we show the resulting $(\pi^{+}\pi^{-})$ mass spectra, which exhibit a peak in the mass region of the ρ meson. To estimate whether this peak is artificially due to the fixed position of the trigger particle in phase space, we calculate a background distribution. This is done by replacing the y-component of the trigger momentum by its negative value and recalculating the mass distributions. These "trigger flip" background distributions peak at the position of the ρ^{o}-mass. We use a second, independent way of constructing the background by combining normal inelastic events (without a high p_T trigger) at random with trigger particles from the high p_T sample. This method yields a background distribution within

statistical fluctuations identical with that obtained by the trigger flip method. We conclude that the low mass correlation peaking around the ρ^o-mass in the background distributions also given in fig. 12, is generated by a conspiracy between trigger bias, kinematical cuts and acceptance properties. For the determination of the ρ^o-signal exceeding the background in our data we used both background distributions in parallel, getting nearly identical results.

A relativistic P-wave Breit-Wigner function has been used to parametrize the effective mass distribution in the ρ region. The production of the ρ^o-meson in the limited phase space region of interest was described by a simple parametrization of the p_T and y dependence of the production cross section, the y-distribution was taken from global fits to ISR measurements [11], while the p_T distribution has been taken from a parametrization of measurements of the British-Scandinavian Collaboration [12]. The ρ^o meson decay angular distribution was assumed to be isotropic. Using a simulation method the decay pions were traced through the detector and the fraction of ρ^o-meson decays was determined in which the π-meson of the right charge fulfilled the trigger conditions and the other one was accepted by the detector. The resulting distorted resonance signal together with the background signal were fitted to the mass distributions in order to determine the number of produced ρ^o-mesons (fig. 12 (a,b)). The results are collected in table 2. The production rate then is compared with directly produced π mesons. The acceptance of the trigger for directly produced π-mesons was calculated using the same parametrisation for π meson production cross section and for ρ^o-mesons.

The possible influence of ω-meson decay on our (π_T^-, π^+) effective mass distributions has also been investigated by simulation methods. Assuming equal production rates for ρ^o - and ω-mesons, we find that the contribution from ω-mesons is at least one order of magnitude smaller than the contribution from ρ^o decay. This is understandable because the ω-meson decays into three π-mesons which makes it kinematically much more difficult for one of them to fulfill the trigger condition.

We conclude that our data can be explained if fragmentation of proton valence quarks yields a ρ/π ratio near unity.

5. AWAY JET PROPERTIES

We assume that the fragment with the largest fraction of momentum of the scattered parton exhibits the original quantum numbers. In particular the average charge of the fastest particle in the away jet is expected to reflect the average charge of the scattered partons [13].

To exclude that the leading particle in the away jet is an undetected neutral, transverse momentum balance has to be estimated. For this purpose we calculate the quantities Σp_x^{tow} and Σp_x^{away} which are the sum of transverse momenta in the trigger plane for charged particles in the towards and away azimuthal range respectively (see fig. 2). The summation is restricted on the towards side to particles within $\Delta y = \pm 0.7$ around the trigger, in the away hemisphere around the charged secondary with largest p_x (jet leader). Defining $x_J = \Sigma p_x^{away}/\Sigma p_x^{tow}$ we obtain a measure for the fraction of the trigger jet transverse momentum compensated by the away side charged particles. Here we use the sample of events with a charged particle trigger at $\theta \simeq 45^o$.

We determine the average charge $\langle q_F \rangle$ of the jet leaders in our sample as a function of x_J. The resulting distributions are shown in fig. 13.

As can be seen in fig. 13(a), the average charge of the largest momentum charged particle increases with x_J and reaches a value of $\frac{1}{3}$ for $x_J \to 1$, i.e. when the trigger jet is balanced by the charged particles of the away jet. Fig. 13(a) contains data for the sum of negative and positive trigger particles and also the separate distributions. We observe, that the dependence of $\langle q_F \rangle$ on x_J does not depend on the trigger charge.

Only events with a back-to-back configuration contribute to fig. 13(a), i.e. where the jet leader with rapidity y_F is in the rapidity hemisphere opposite to the trigger ($y^{(t)} \simeq + 0.8$).

In a simple valence quark parton model a value of $\langle q_F \rangle = \frac{1}{3}$ is expected, since the average quark charge in a proton is $\langle q \rangle = \Sigma q_i/\text{number of quarks}$ in proton = 1/3. The independence of the result from the trigger charge then is an indication for gluon exchange mediating the large p_T process.

Resulting distributions for events where the jet leader of the away jet and the trigger are in the same rapidity hemisphere are displayed in fig. 13(b).

The behaviour of $\langle q_F \rangle$ of fig. 13(b) is possibly due to the fact that this configuration results from the participation of partons of low x in the hard scattering process. Hence the inclusion of sea quarks and gluons in addition to valence quarks will alter and decrease the simple prediction $\langle q_F \rangle = 1/3$.

6. CONCLUSION

Using parton fragmentation properties, we explain the behaviour of the four jets originating in a large p_T event. Analyzing a data sample with the asymmetrical trigger condition $\theta = 20^o$, the two spectator jets are attributed either to the same proton as the trigger or to the other. We observe no correlation between the nature of the trigger particle and the charge composition of the spectator jet in the opposite rapidity hemisphere. On the other hand, a number of very specific predictions for correlations between nature of the trigger particle and the spectator jet on the same rapidity side is verified. The distribution of charged particle in reduced longitudinal momentum x' in the rest frame of the two spectators is well described by a power law $(1 - x')^n$. All distributions show the behaviour expected from dimensional counting rules, if we allow for an extra power for d quark fragmentation. In contrast to a simple quark scattering picture, we are led to infer that the triggering large p_T protons originate from a fragmenting diquark system.

As to the production ratio of direct pions to ρ^o mesons we obtain a ratio near unity (for equal transverse momenta in the region of 2 GeV/c), in accordance with expectation and observation in deep inelastic lepton scattering.

Finally, the average charge of the fastest particle in the away side jet equals the average charge of the valence quarks of a proton. This is the case in a configuration where valence quarks dominate and the result does not depend on the charge of the trigger.

Acknowledgement

We have greatly profited from discussions with Professors S. Brodsky, H. Genz, M. Schmidt, W. Schmidt, W. Ochs, J. Wess. The Heidelberg and Karlsruhe groups were supported by a grant from the Bundesministerium für Forschung und Technologie of the Federal Republic of Germany, the Collège de France group was supported by the IN2P3.

REFERENCES

[1] CCHK Collaboration, M. Della Negra et al., Nucl. Phys. B127 (1977) 1.

[2] R.P. Feynman, Photon hadron interactions, New York, 1972;
R.D. Field and R.P. Feynman, Phys. Rev. D15 (1977) 2590;
R.P. Feynman, R.D. Field and G.C. Fox, Nucl. Phys. B128 (1977) 1.

[3] M. Sehgal, in Proceedings of Lepton Photon Conference Hamburg 1977.

[4] S.J. Brodsky and G.R. Farrar, Phys. Rev. Lett. 31 (1973) 1153.

[5] P. Hanke, thesis Karlsruhe 1976, Kernforschungszentrum Karlsruhe report KfK 2412 (1977).

[6] CHLM Collaboration, M. Albrow et al., Nucl. Phys. B56 (1973) 333;
CHLM Collaboration, M. Albrow et al., Nucl. Phys. B73 (1974) 40.

[7] CCHK Collaboration, M. Della Negra et al., Phys. Lett. 59B (1975) 81.

[8] M. Jacob and P.V. Landshoff, Nucl. Phys. B113 (1976) 395.

[9] F.C. Erné and J.C. Sens, CERN preprint, submitted to Phys. Rev. Lett.

[10] I. Cohen et al., DESY 77/71 and DESY 78/12.

[11] P. Capiluppi et al., Nucl. Phys. B79 (1974) 189.

[12] B. Alper et al., Nucl. Phys. B87 (1975) 19.

[13] R.D. Field and R.P. Feynman, Nucl. Phys. B156 (1978) 1.

TABLE 1

Trigger type	Spectator fragment type	fragmentation function "counting rules"
p	π^+	$(1 - x)$
p	π^-	$(1 - x)^2$
π^+	p	$(1 - x)$
π^+	π^-	$(1 - x)^4$
π^-	p	$(1 - x)$
π^-	π^-	$(1 - x)^7$
K^-	p	$(1 - x)$
K^-	π^-	$(1 - x)^8$

TABLE 2

Trigger type	π^-	π^+
Number of triggers	14 000	28 000
$\langle p_T \rangle$	1.7 GeV/c	2.5 GeV/c
Number of ρ^o observed	313 ± 44	1164 ± 64
ρ^o/π^- resp. π^+	0.82 ± 0.15	1.34 ± 0.15

TABLE CAPTIONS

Table 1 Fragmentation functions for the same rapidity spectator jet for different trigger particles, derived from dimensional counting rules with vector gluon exchange.

Table 2 Properties of trigger jet sample used for determination of the ρ/π ratio.

FIGURE CAPTIONS

Fig. 1 Pictorial representation of the quark-quark scattering process leading to a four-jet structure in a large p_T event.

Fig. 2 Coordinate system, indicating the different kinematical regions.

Fig. 3 Ratio of the number of secondaries for a π^- trigger to secondaries for a π^+ trigger:
(i) For positive secondaries.
(ii) For negative secondaries.

Fig. 4 Same as fig. 3 for p to π^+ trigger.

Fig. 5 Same as fig. 3 for K^- to π^- trigger.

Fig. 6 Particle density of positive secondaries in the spectator jet accompanying a triggering proton as a function of $(1 - x')$, x' being the reduced longitudinal momentum in the jet.

Fig. 7 Particle density of positive particles in the spectator jet accompanying the triggering pion as a function of $(1 - x')$.

Fig. 8 Particle density of negative particles in the spectator jet accompanying the triggering π^+ as a function of $(1 - x')$.

Fig. 9 Ratio of particle densities of positive and negative secondaries for a π^- trigger to a π^+ trigger as a function of $(1 - x')$.

Fig. 10 Ratio of particle densities of positive and negative secondaries in the spectator jet for a K^- trigger to a π^- trigger versus $(1 - x')$.

Fig. 11 Ratio of particle densities of negative to positive secondaries in the spectator jet accompanying a triggering proton versus $(1 - x')$.

Fig 12 Invariant $\pi^+\pi^-$ mass spectrum for the trigger jet (full line): (a) π^+ is a large p_T trigger and (b) π^- is a large p_T trigger. The dotted curve is an estimate of the background; the hatched is the sum of background and Breit-Wigner distribution for the ρ meson.

Fig. 13 Mean charge of the jet leader in the away jet as a function of x_J, the fraction of transverse momentum compensated by charged particles:

(a) trigger jet and away jet back-to-back in rapidity, for positive and negative trigger particles and for the combined sample;

(b) trigger jet and away jet back-anti-back in rapidity, for positive and negative trigger particles and for the combined sample.

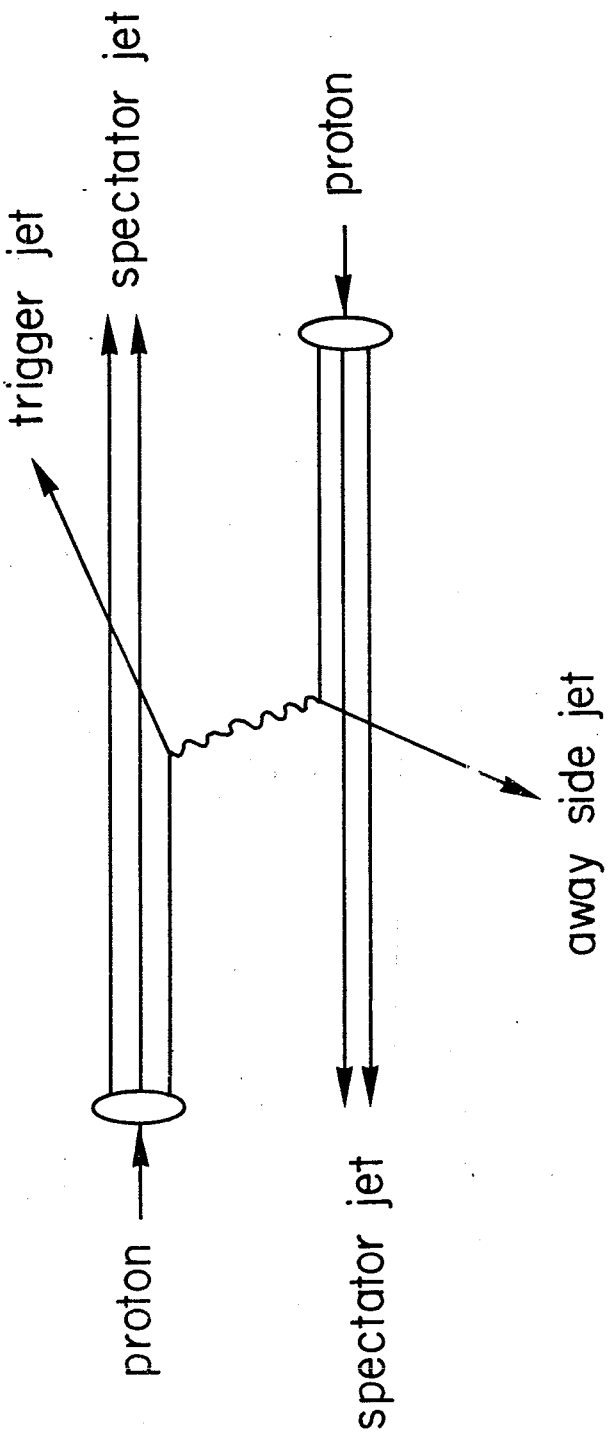
trigger jet
spectator jet
proton
away side jet
proton
spectator jet

Fig. 1

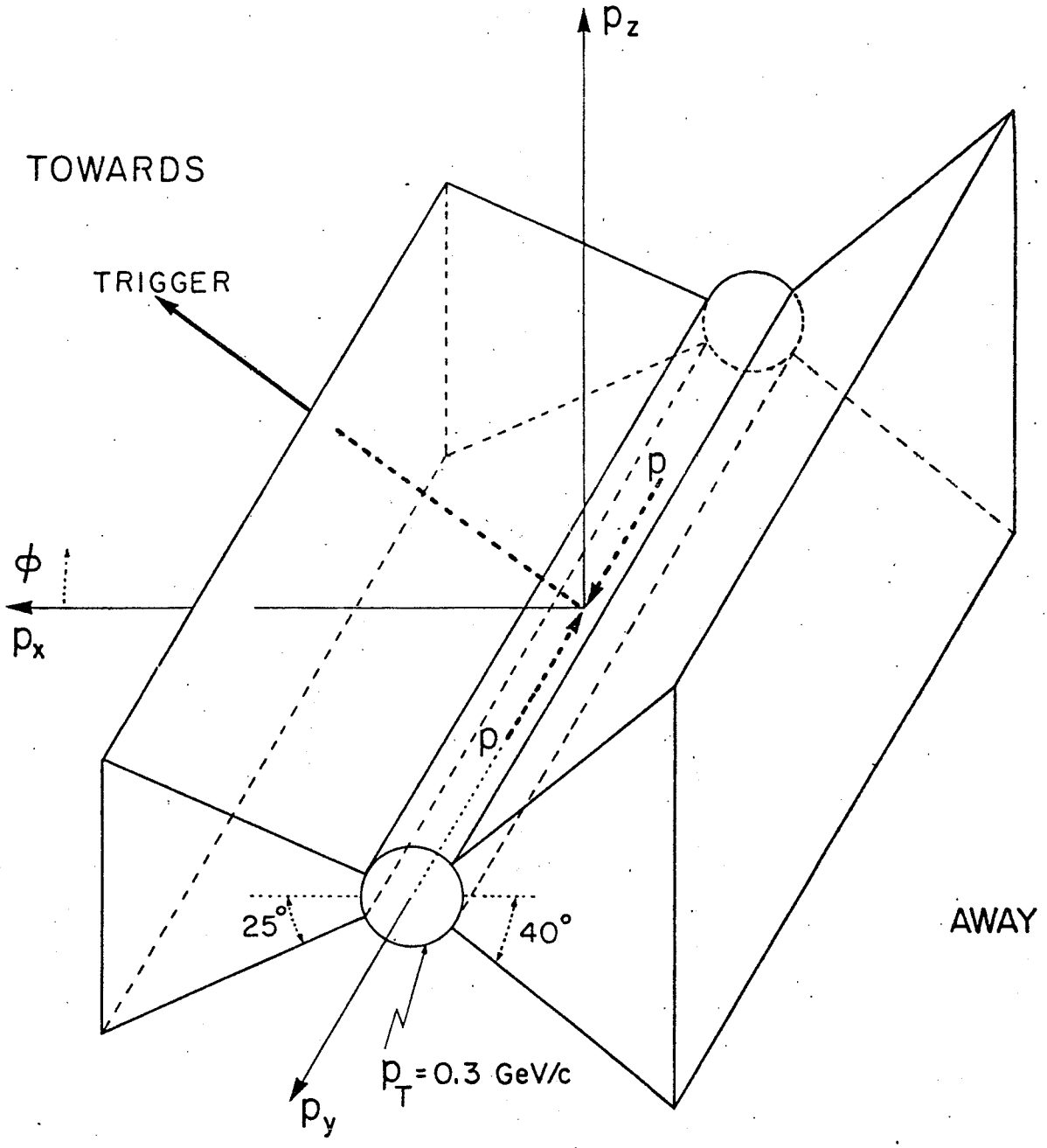

Fig. 2

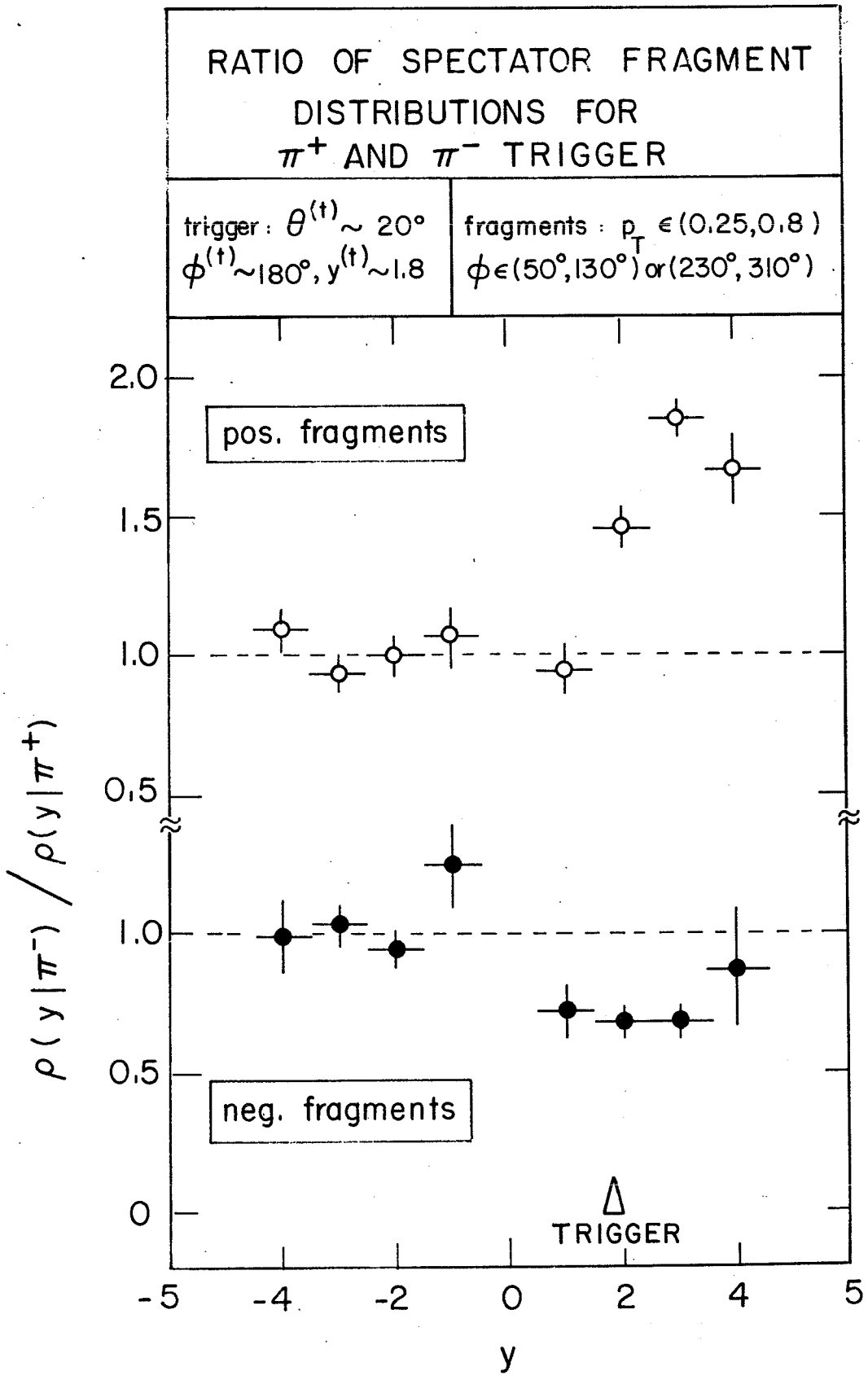
RATIO OF SPECTATOR FRAGMENT DISTRIBUTIONS FOR π^+ AND π^- TRIGGER
trigger : $\theta^{(t)} \sim 20°$
$\phi^{(t)} \sim 180°$, $y^{(t)} \sim 1.8$
fragments : $p_T \in (0.25, 0.8)$
$\phi \in (50°, 130°)$ or $(230°, 310°)$
pos. fragments
neg. fragments
TRIGGER
$\rho(y|\pi^-) / \rho(y|\pi^+)$
y
2.0
1.5
1.0
0.5
1.0
0.5
0
-5
-4
-2
0
2
4
5

Fig. 3

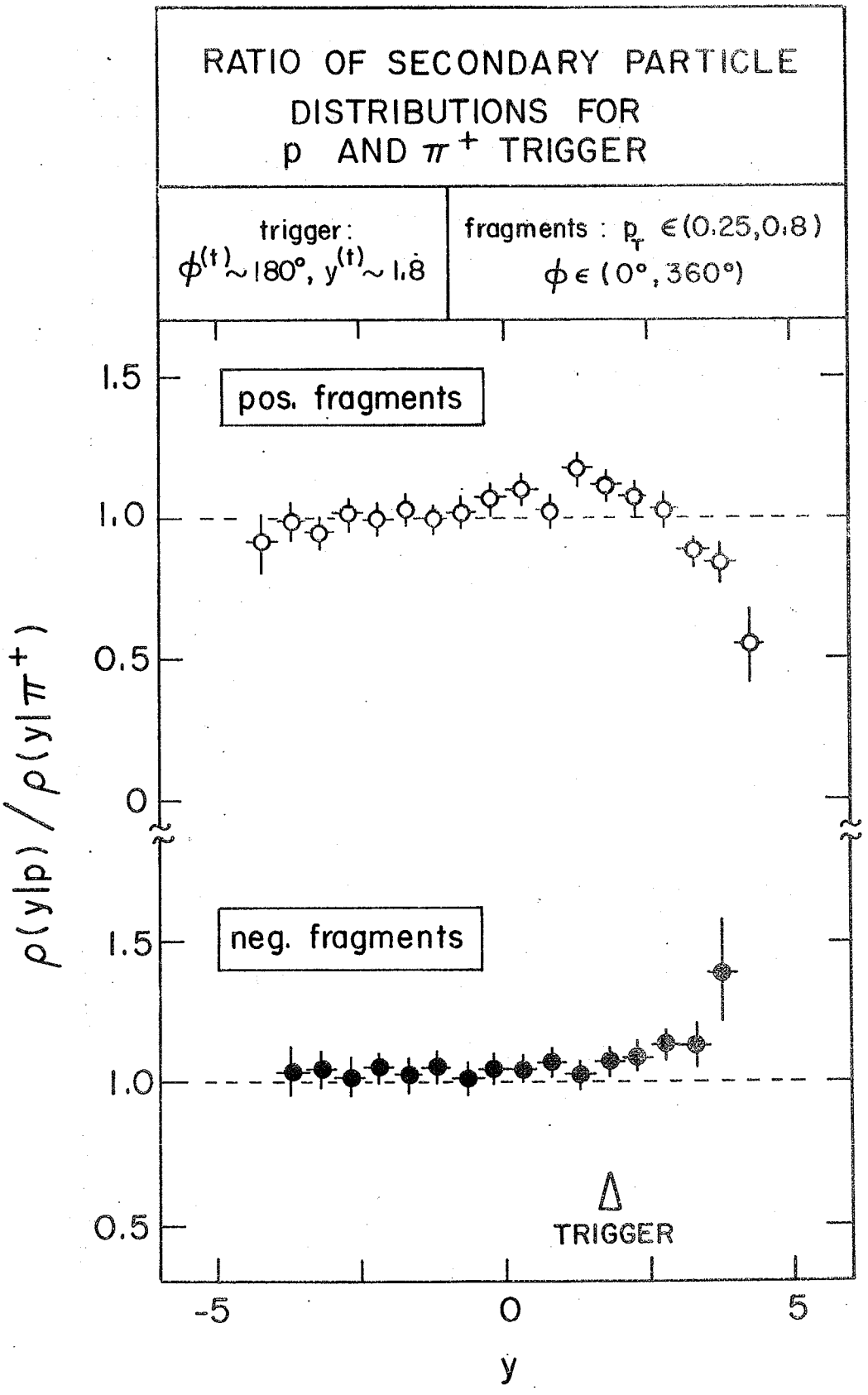
RATIO OF SECONDARY PARTICLE DISTRIBUTIONS FOR p AND π+ TRIGGER
trigger: φ(t) ~ 180°, y(t) ~ 1.8
fragments : pT ∈ (0.25, 0.8) φ ∈ (0°, 360°)
pos. fragments
neg. fragments
TRIGGER
ρ(y|p) / ρ(y|π+)
y
1.5
1.0
0.5
0
-5
5

Fig. 4

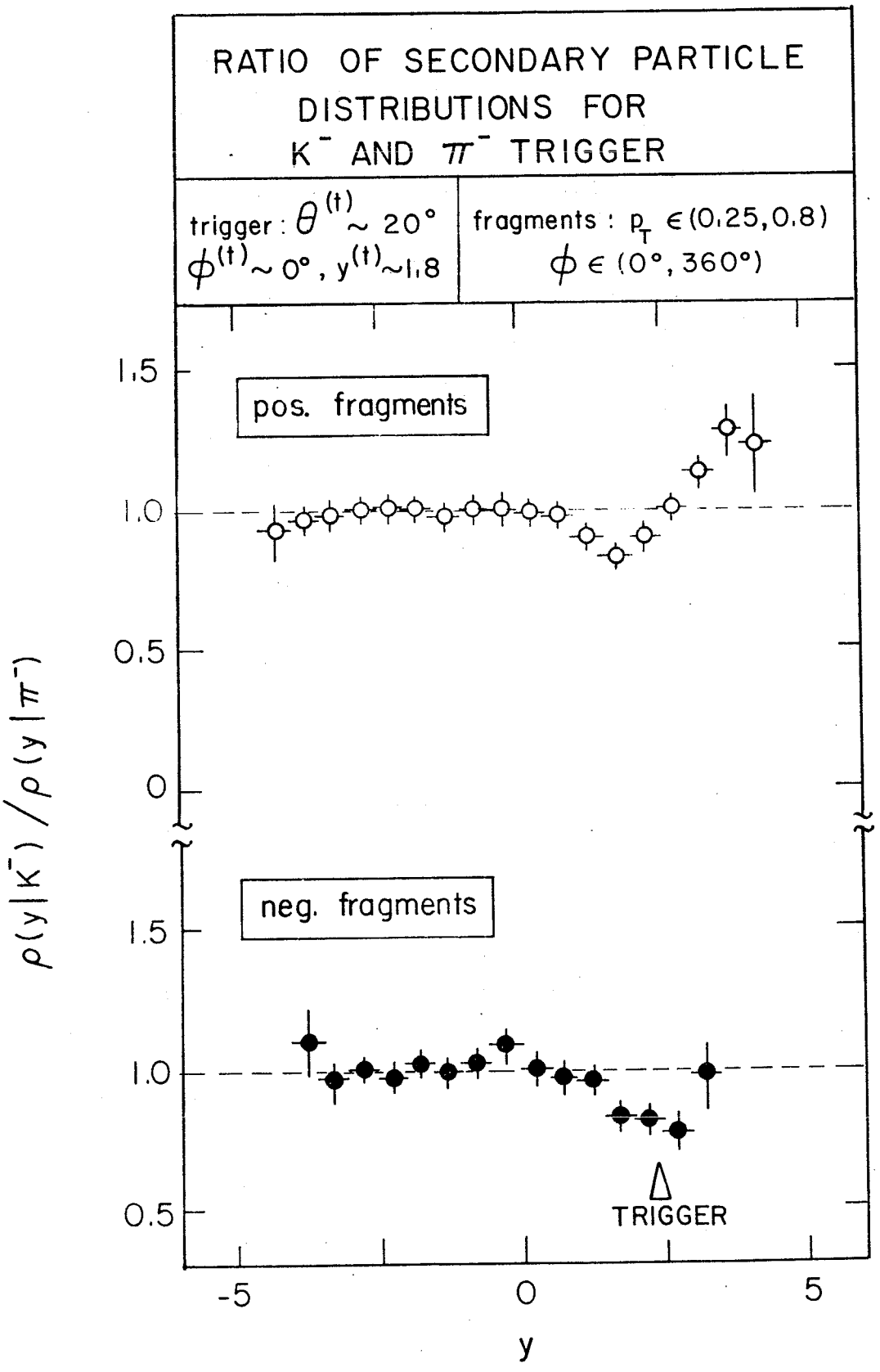
RATIO OF SECONDARY PARTICLE DISTRIBUTIONS FOR K⁻ AND π⁻ TRIGGER
trigger : θ(t) ~ 20°
φ(t) ~ 0°, y(t) ~ 1.8
fragments : pT ∈ (0.25, 0.8)
φ ∈ (0°, 360°)
pos. fragments
neg. fragments
TRIGGER
ρ(y|K⁻) / ρ(y|π⁻)
y
1.5
1.0
0.5
0
-5
0
5

Fig. 5

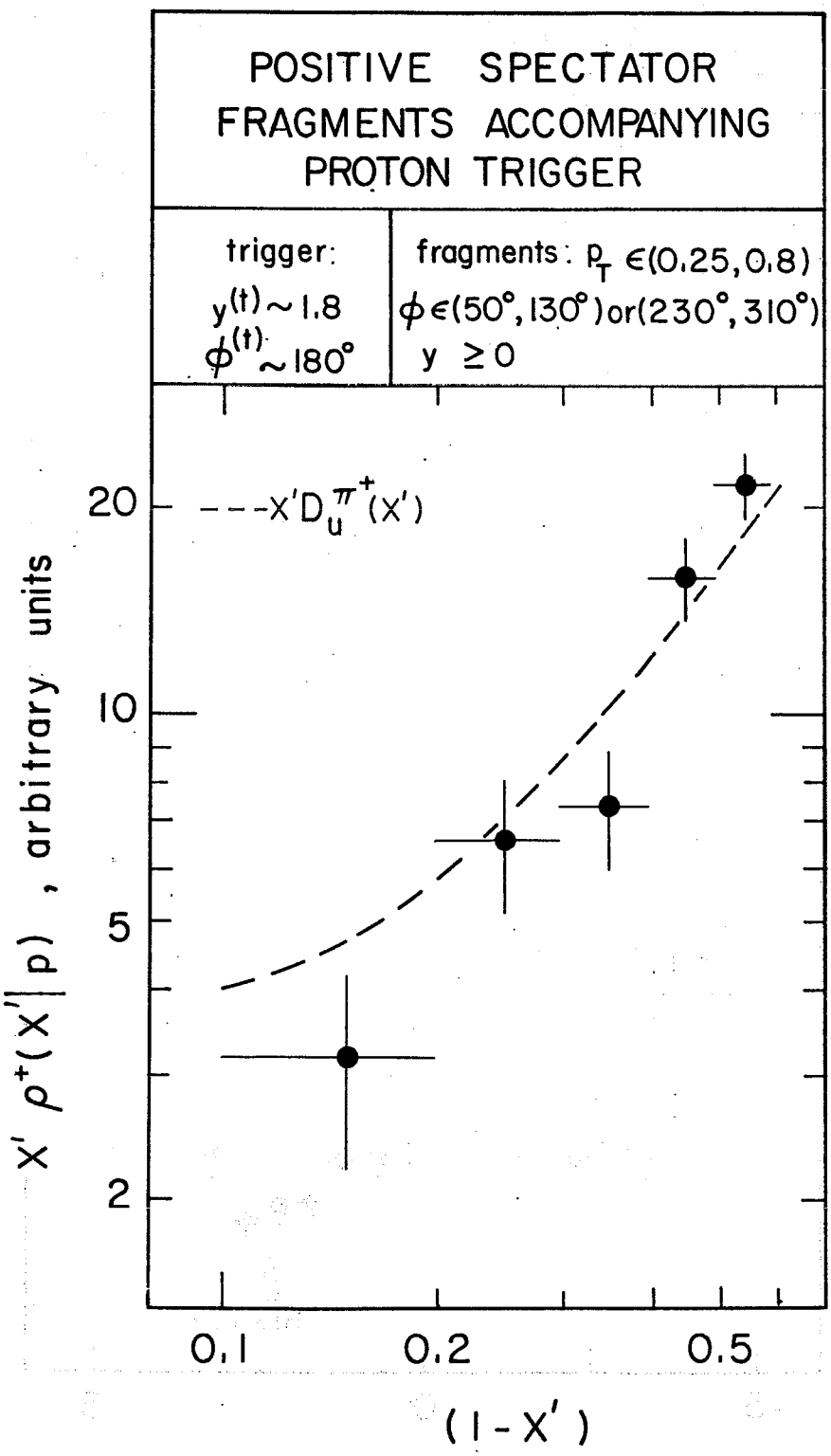
POSITIVE SPECTATOR
FRAGMENTS ACCOMPANYING
PROTON TRIGGER
trigger:
$y^{(t)} \sim 1.8$
$\phi^{(t)} \sim 180°$
fragments: $p_T \in (0.25, 0.8)$
$\phi \in (50°, 130°)$ or $(230°, 310°)$
$y \geq 0$
$---X' D_u^{\pi^+}(X')$
$X'\rho^+(X'|p)$, arbitrary units
20
10
5
2
0.1
0.2
0.5
$(1-X')$

Fig. 6

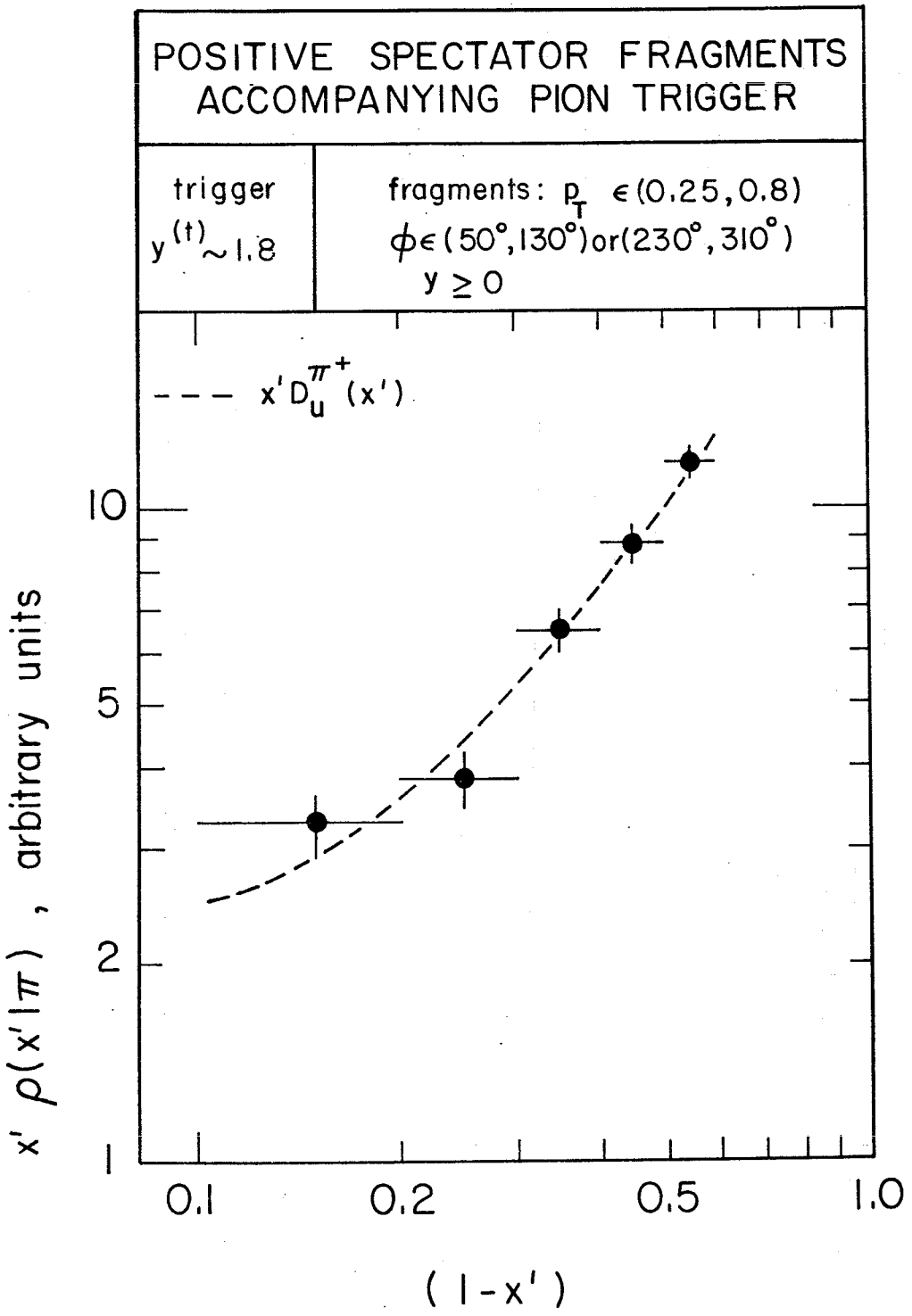
POSITIVE SPECTATOR FRAGMENTS
ACCOMPANYING PION TRIGGER
trigger
$y^{(t)} \sim 1.8$
fragments: $p_T \in (0.25, 0.8)$
$\phi \in (50°, 130°)$ or $(230°, 310°)$
$y \geq 0$
--- $x' D_u^{\pi^+}(x')$
$x'\rho(x'|\pi)$, arbitrary units
10
5
2
1
0.1
0.2
0.5
1.0
$(1-x')$

Fig. 7

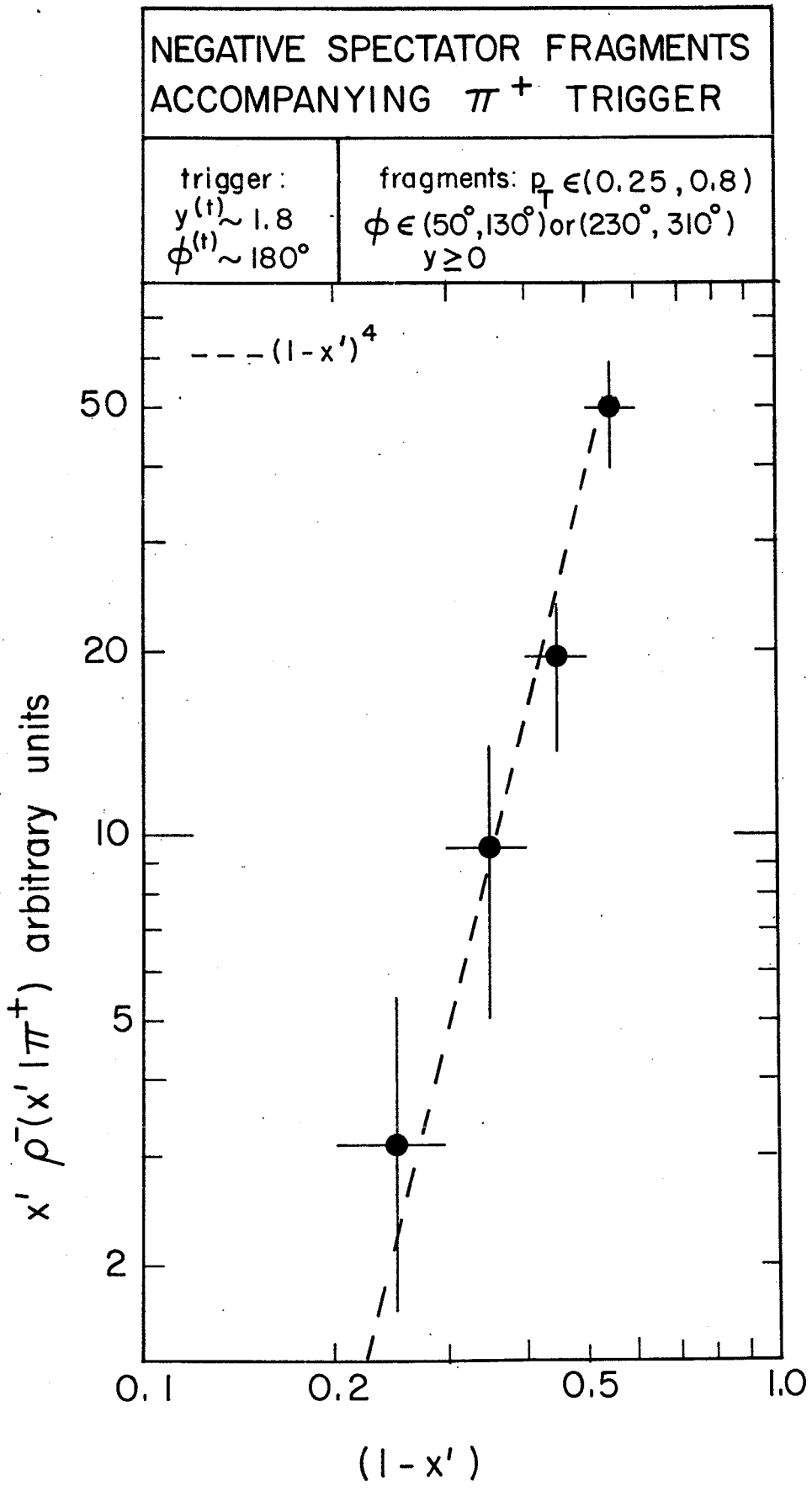
NEGATIVE SPECTATOR FRAGMENTS
ACCOMPANYING π^+ TRIGGER
trigger:
$y^{(t)} \sim 1.8$
$\phi^{(t)} \sim 180°$
fragments: $p_T \in (0.25, 0.8)$
$\phi \in (50°, 130°)$ or $(230°, 310°)$
$y \geq 0$
$---(1-x')^4$
50
20
10
5
2
$x'\,\rho^-(x'|\pi^+)$ arbitrary units
0.1
0.2
0.5
1.0
$(1-x')$

Fig. 8

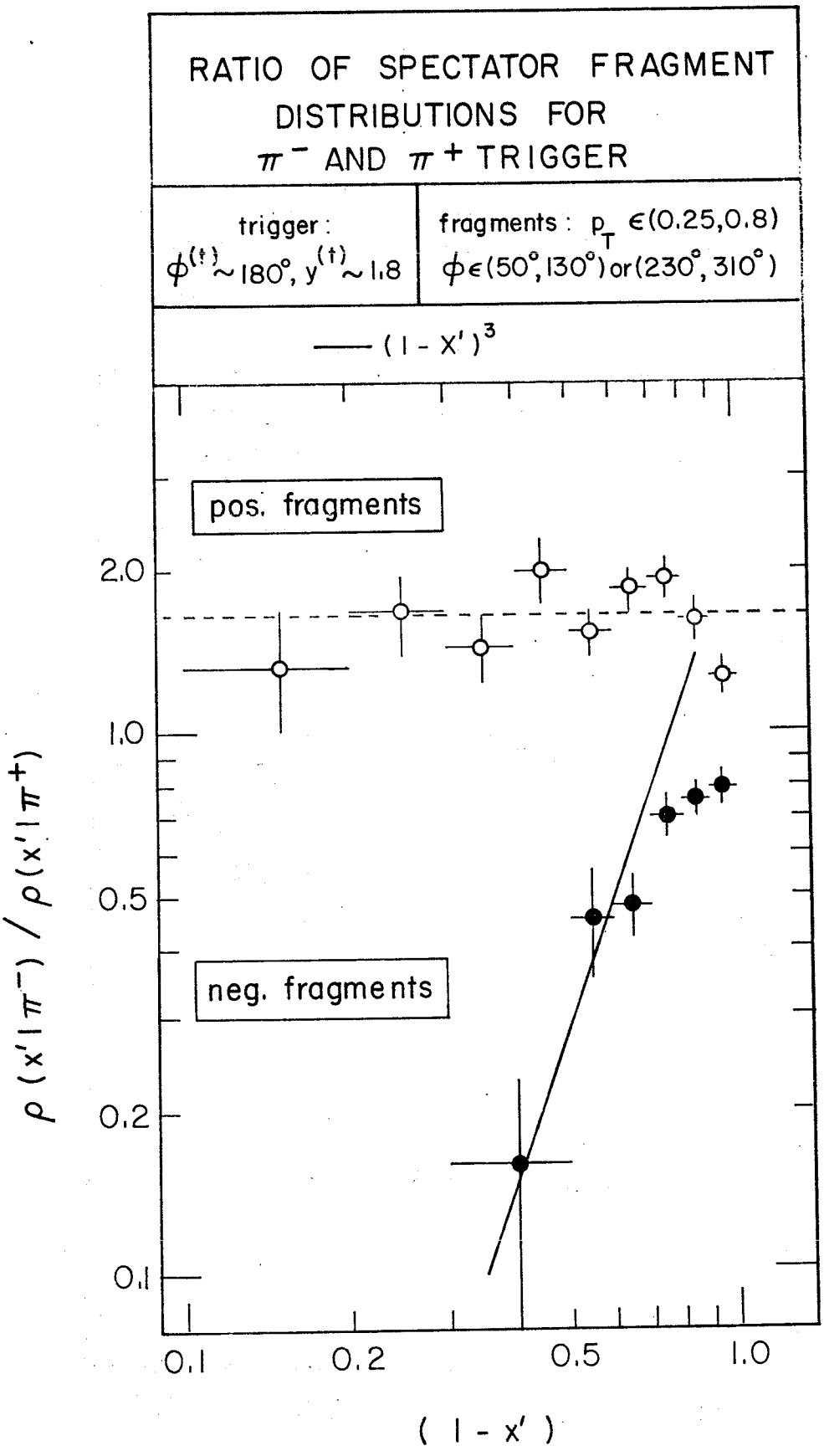
RATIO OF SPECTATOR FRAGMENT DISTRIBUTIONS FOR
π⁻ AND π⁺ TRIGGER
trigger :
φ(t) ~ 180°, y(t) ~ 1.8
fragments : pT ∈(0.25,0.8)
φ ∈(50°,130°) or (230°,310°)
—— (1 - X')³
pos. fragments
neg. fragments
ρ (x'1π⁻) / ρ (x'1π⁺)
2.0
1.0
0.5
0.2
0.1
0.1
0.2
0.5
1.0
(1 - x')

Fig. 9

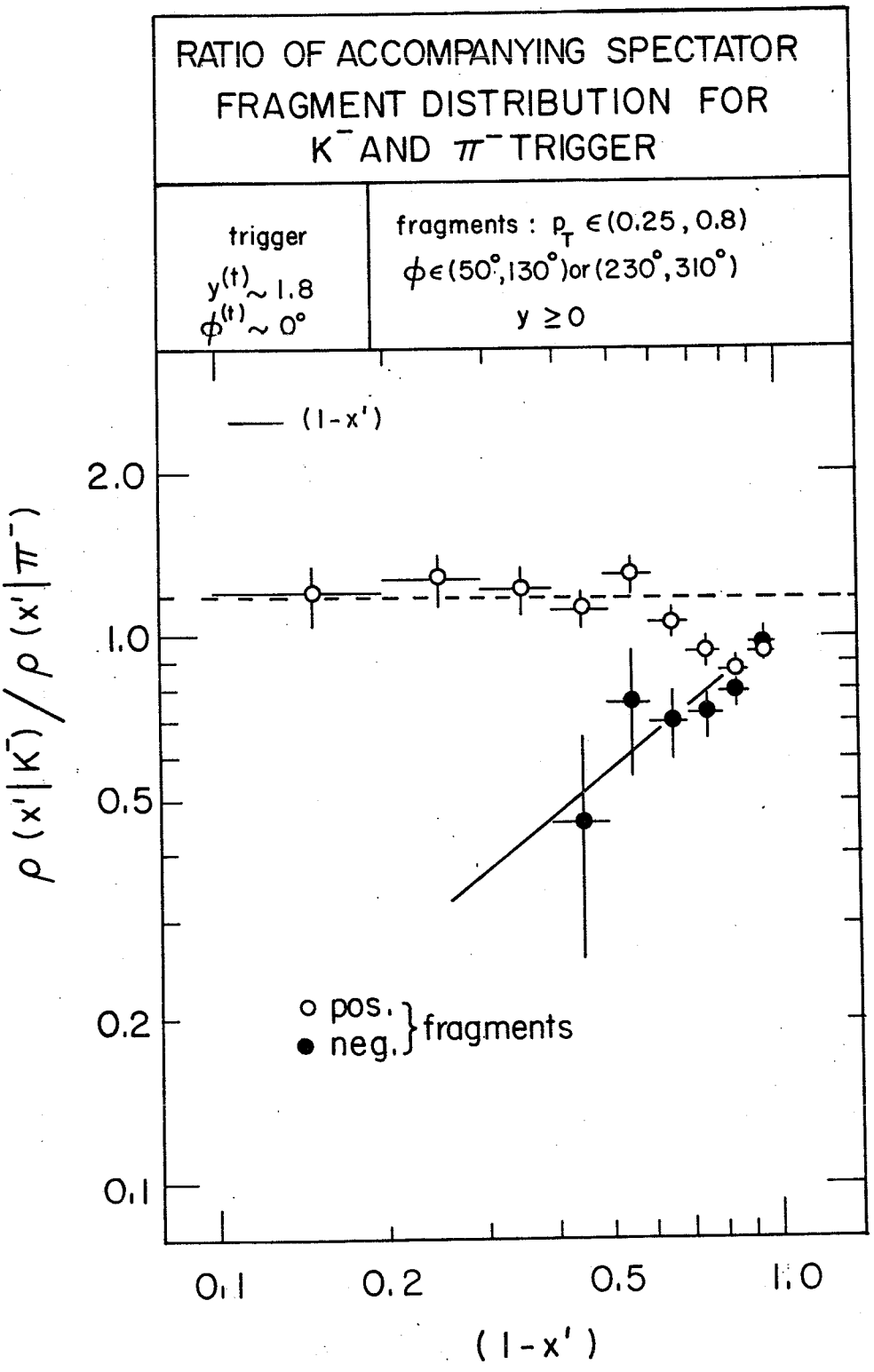
RATIO OF ACCOMPANYING SPECTATOR FRAGMENT DISTRIBUTION FOR K⁻ AND π⁻ TRIGGER
trigger
y(t) ~ 1.8
φ(t) ~ 0°
fragments : pT ∈ (0.25, 0.8)
φ ∈ (50°, 130°) or (230°, 310°)
y ≥ 0
(1-x')
ρ (x'|K⁻) / ρ (x'|π⁻)
2.0
1.0
0.5
0.2
0.1
o pos.
● neg.
} fragments
0.1
0.2
0.5
1.0
(1-x')

Fig. 10

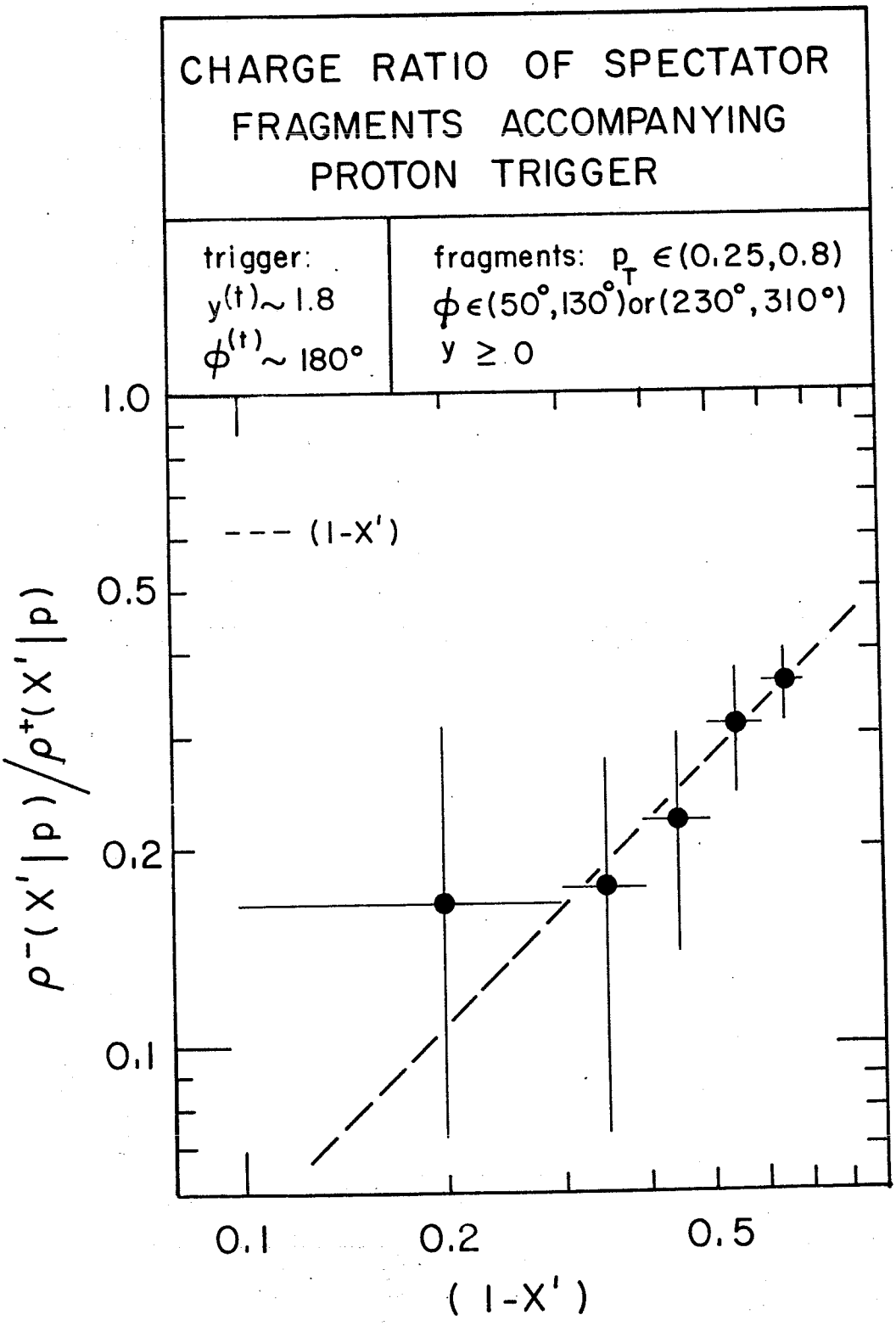
CHARGE RATIO OF SPECTATOR FRAGMENTS ACCOMPANYING PROTON TRIGGER
trigger:
$y^{(t)} \sim 1.8$
$\phi^{(t)} \sim 180°$
fragments: $p_T \in (0.25, 0.8)$
$\phi \in (50°, 130°)$ or $(230°, 310°)$
$y \geq 0$
--- (1-X')
$\rho^-(X'|p)/\rho^+(X'|p)$
1.0
0.5
0.2
0.1
0.1
0.2
0.5
(1-X')

Fig. 11

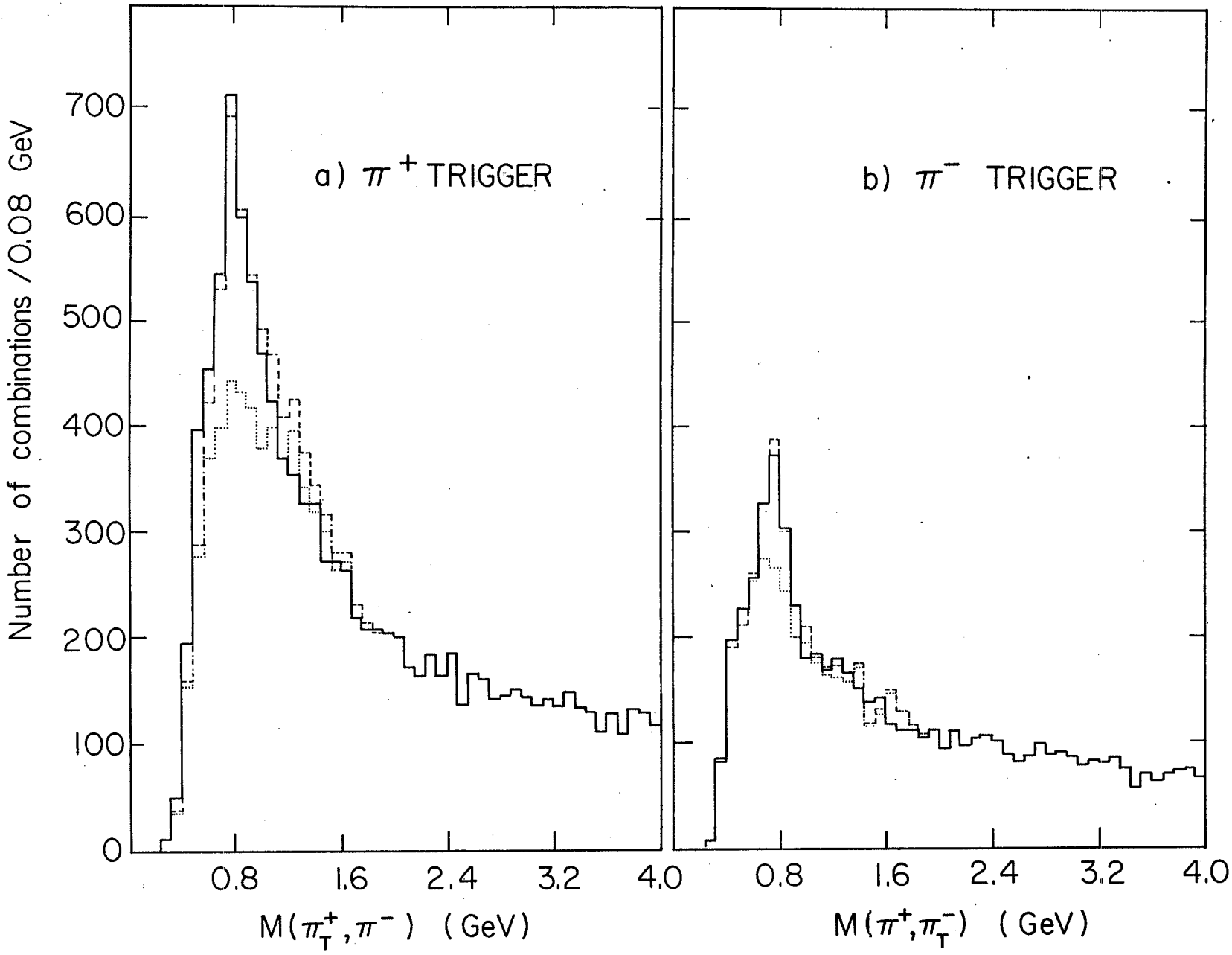
a) π^+ TRIGGER
b) π^- TRIGGER
Number of combinations /0.08 GeV
0
100
200
300
400
500
600
700
0.8
1.6
2.4
3.2
4.0
$M(\pi_T^+, \pi^-)$ (GeV)
$M(\pi^+, \pi_T^-)$ (GeV)

Fig. 12

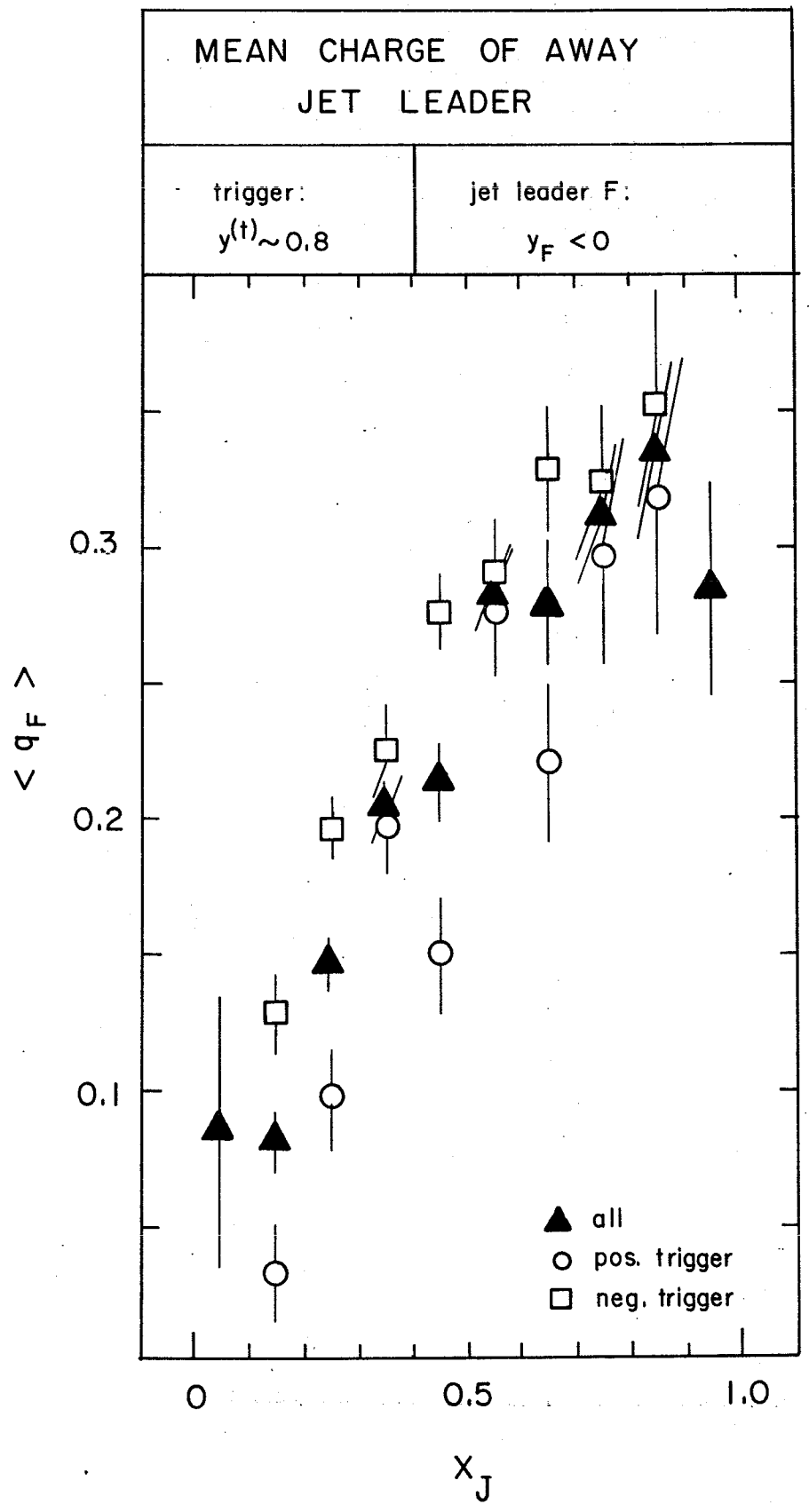
MEAN CHARGE OF AWAY JET LEADER
trigger:
$y^{(t)} \sim 0.8$
jet leader F:
$y_F < 0$
$< q_F >$
0.3
0.2
0.1
0
0.5
1.0
x_J
all
pos. trigger
neg. trigger

Fig 13(a)

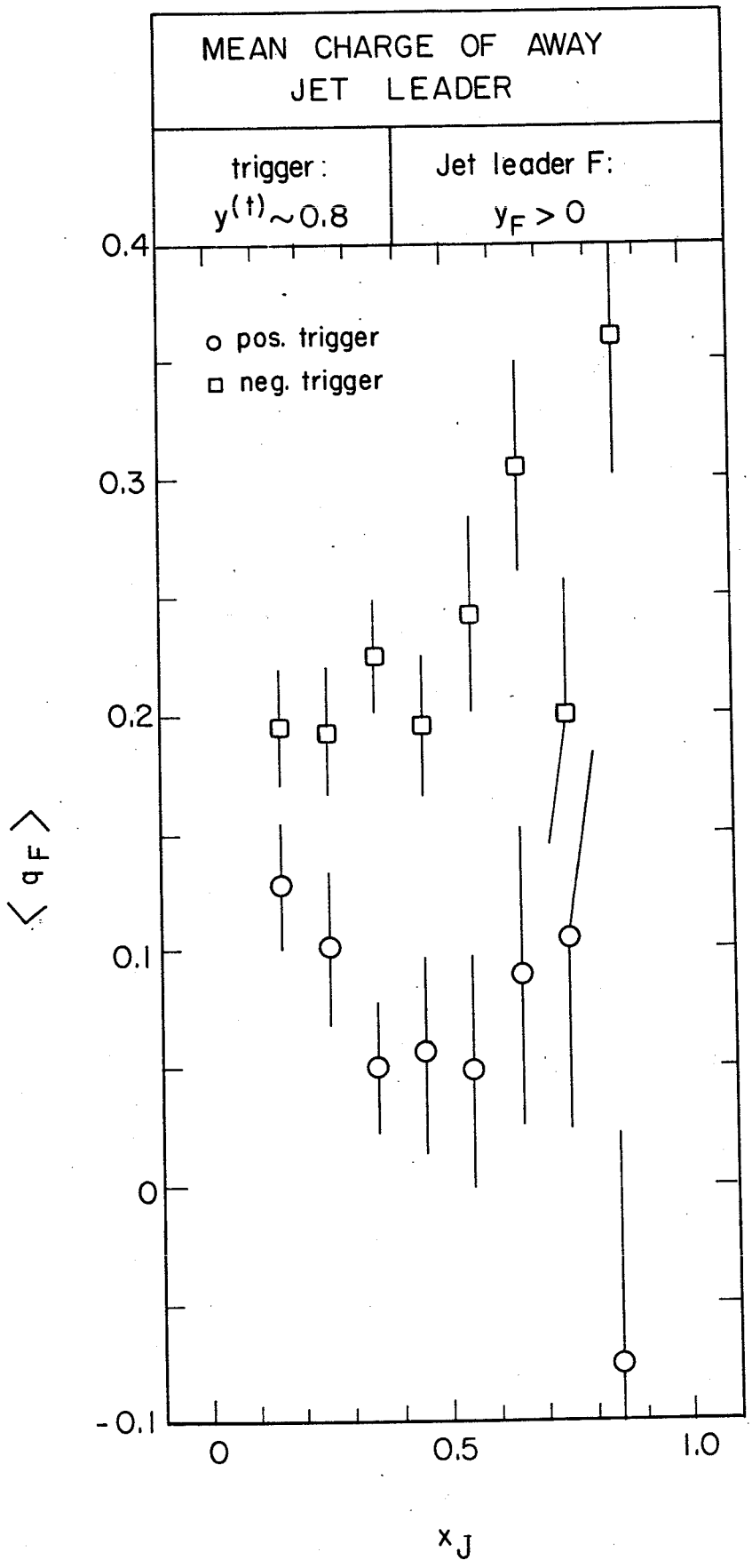
MEAN CHARGE OF AWAY JET LEADER
trigger: $y^{(t)} \sim 0.8$
Jet leader F: $y_F > 0$
o pos. trigger
□ neg. trigger
0.4
0.3
0.2
0.1
0
-0.1
0
0.5
1.0
$\langle q_F \rangle$
x_J

Fig 13(b)